Acoustic phonon scattering limited carrier mobility in two-dimensional extrinsic graphene

E. H. Hwang and S. Das Sarma

Condensed Matter Theory Center, Department of Physics, University of Maryland, College Park, Maryland 20742-4111, USA

We theoretically calculate the phonon scattering limited electron mobility in extrinsic (i.e., gated or doped with a tunable and finite carrier density) two-dimensional graphene layers as a function of temperature (T) and carrier density (n). We find a temperature-dependent phonon-limited resistivity $\rho_{ph}(T)$ to be linear in temperature for $T \gtrsim 50$ K with the room-temperature intrinsic mobility reaching the values of above 10^5 cm^2/V s. We comment on the low-temperature Bloch–Grüneisen behavior where $\rho_{ph}(T) \sim T^4$ for unscreened electron-phonon coupling.

I. INTRODUCTION

Low-temperature carrier transport properties of two-dimensional (2D) graphene layers have been of great current interest to both experimentalists[1–5] and theorists[6–10] alike ever since the possibility of fabricating stable gated 2D graphene monolayers on SiO$_2$ substrates and measuring the density-dependent conductivity of the 2D chiral graphene carriers were demonstrated.[1] Much of the early interest focused understandably on the important issues of the scattering mechanisms limiting the low-temperature conductivity and the associated graphene "minimal conductivity" at the charge neutral ("Dirac") point. One of the dominant low-temperature scattering mechanisms[3,4,9,10] in graphene is that due to screened Coulomb scattering by unintended charged impurities invariably present in the (mostly SiO$_2$) substrate (and the substrate-graphene interface) although short-range scattering by neutral defects also contributes, particularly at high carrier densities in high-mobility samples. It has therefore been argued[9,10] that gated graphene layers are similar to 2D electron systems in confined semiconductor structures (e.g., Si inversion layers, GaAs heterostructures, and quantum wells), where also long-range charged impurity scattering dominates low-temperature Ohmic transport with short-range (e.g., interface roughness) scattering playing a role at high carrier densities.[11,12]

Given the exciting technological context of graphene as a prospective electronic transistor material for future applications, the question therefore naturally arises about the limiting value of the *intrinsic* room-temperature graphene mobility if all extrinsic scattering mechanisms, e.g., charged impurities, neutral defects, interface roughness, graphene ripples, etc., can be eliminated from the system. This question is more than of academic interest since serious experimental efforts are underway[13] to eliminate charged impurities from graphene by using different substrates or by working with freestanding graphene layers without any substrates. It is also noteworthy that the systematic elimination of charged impurity scattering through modulation doping and material improvement in the molecular beam epitaxy growth technique has led to an astonishing 3000-fold enhancement in the low-temperature 2D GaAs electron mobility from 10^4 cm^2/V s in 1978 to 30×10^6 cm^2/V s in 2000; future enhancement to 100×10^6 cm^2/V s mobility is anticipated[14] in the next few years.

One great advantage of graphene over high-mobility 2D GaAs systems is that the lack of strong long-range polar optical phonon scattering, which completely dominates[15] the room-temperature GaAs mobility ($\sim$2000 cm^2/V s), in graphene should lead to very high intrinsic room-temperature graphene mobility, limited only by the weak deformation-potential scattering from the thermal lattice acoustic phonons. In this work, we calculate the temperature-dependent 2D graphene mobility limited only by the background lattice acoustic phonon scattering. We find that room-temperature intrinsic (i.e., just phonon-limited) graphene mobility surpassing 10^5 cm^2/V s is feasible using the generally accepted values in the literature for the graphene sound velocity and deformation coupling. There is some uncertainty in the precise value of the electron-phonon deformation-potential coupling constant, leading to a concomitant uncertainty in the intrinsic graphene mobility. This situation is similar[16] to the 2D GaAs system where, in fact, precise measurement of the phonon-limited 2D mobility led to the correct deformation-potential coupling for transport studies, and this could be the case for graphene also where a quantitative comparison between our theoretical results presented in this work with the measured temperature-dependent graphene mobility, very recently becoming available,[17,18] could lead to an accurate determination of the graphene electron-phonon deformation-potential coupling constant.

The paper is organized as follows. In Sec. II, the Boltzmann transport theory is presented to calculate acoustic phonon scattering limited 2D graphene conductivity. Section III presents the results of the calculation. In Section IV we discuss the results compared to experimental data, and we conclude in Sec. V.

II. THEORY

We use the Boltzmann transport theory[15,16] to calculate acoustic phonon scattering limited 2D graphene conductivity. We consider only the longitudinal acoustic (LA) phonons in our theory since either the couplings to other graphene lattice phonon modes are too weak or the energy scales of these (optical) phonon modes are far too high for them to provide an effective scattering channel in the temperature range (5–500 K) of our interest.

The conductivity of graphene is given by

$$\sigma = e^2 D(E_F) \frac{v_F^2}{2} \langle \tau \rangle, \tag{1}$$

where v_F is the Fermi velocity, $D(E_F) = (g_s g_v / 2\pi\hbar^2) E_F / v_F^2$ is the density of states of graphene at the Fermi level (E_F), and $\langle \tau \rangle$ is the relaxation time averaged over energy, i.e.,

$$\langle \tau \rangle = \frac{\int d\varepsilon D(\varepsilon) \tau(\varepsilon) \left[-\dfrac{df(\varepsilon)}{d\varepsilon} \right]}{\int d\varepsilon D(\varepsilon) \left[-\dfrac{df(\varepsilon)}{d\varepsilon} \right]}, \tag{2}$$

where $f(\varepsilon)$ is the Fermi distribution function, $f(\epsilon_k) = \{1 + \exp[\beta(\epsilon_k - \mu)]\}^{-1}$, with $\beta = 1/k_B T$ and $\mu(T, n)$ as the finite temperature chemical potential determined self-consistently. The energy dependent relaxation time $[\tau(\varepsilon_k)]$ is defined by

$$\frac{1}{\tau(\varepsilon_k)} = \sum_{k'} (1 - \cos\theta_{kk'}) W_{kk'} \frac{1 - f(\varepsilon')}{1 - f(\varepsilon)}, \tag{3}$$

where $\theta_{kk'}$ is the scattering angle between k and k', $\varepsilon = \hbar v_F |k|$, and $W_{kk'}$ is the transition probability from the state with momentum k to k' state. In this paper, we only consider the relaxation time due to deformation-potential coupled acoustic phonon mode. The deformation potential due to quasistatic deformation of lattice is taken into account. Then, the transition probability has the form

$$W_{kk'} = \frac{2\pi}{\hbar} \sum_q |C(q)|^2 \Delta(\varepsilon, \varepsilon'), \tag{4}$$

where $C(q)$ is the matrix element for scattering by acoustic phonon and $\Delta(\varepsilon, \varepsilon')$ is given by

$$\Delta(\varepsilon, \varepsilon') = N_q \delta(\varepsilon - \varepsilon' + \omega_q) + (N_q + 1) \delta(\varepsilon - \varepsilon' - \omega_q), \tag{5}$$

where $\omega_q = v_{ph} q$ is the acoustic phonon energy with v_{ph} being the phonon velocity and N_q is the phonon occupation number,

$$N_q = \frac{1}{\exp(\beta \omega_q) - 1}. \tag{6}$$

The first (second) term in Eq. (5) corresponds to the absorption (emission) of an acoustic phonon of wave vector $q = k - k'$. The matrix element $C(q)$ is independent of the phonon occupation numbers. The matrix element $|C(q)|^2$ for the deformation potential is given by

$$|C(q)|^2 = \frac{D^2 \hbar q}{2A \rho_m v_{ph}} \left[1 - \left(\frac{q}{2k} \right)^2 \right], \tag{7}$$

where D is the deformation-potential coupling constant, ρ_m is the graphene mass density, and A is the area of the sample.

The scattering of electrons by acoustic phonons may be considered quasielastic since $\hbar \omega_q \ll E_F$, where E_F is the Fermi energy. There are two transport regimes, which apply to the temperature regimes $T \ll T_{BG}$ and $T \gg T_{BG}$, depending on whether the phonon system is degenerate [Bloch-Grüneisen (BG)] or nondegenerate [equipartition (EP)]. The characteristic temperature T_{BG} is defined as $k_B T_{BG} = 2 k_F v_{ph}$, which is given, in graphene, by $T_{BG} = 2 v_{ph} k_F / k_B \approx 54\sqrt{n}$ K with density measured in unit of $n = 10^{12}$ cm^{-2}. First, we consider $\hbar \omega_q \ll k_B T$. In this case, we have $N_q \sim k_B T / \hbar \omega_q$ and $\Delta(\varepsilon, \varepsilon') = (2 k_B T / \hbar \omega_q) \delta(\varepsilon - \varepsilon')$. Then, the relaxation time is calculated to be

$$\frac{1}{\tau(\varepsilon_k)} = \frac{1}{\hbar^3} \frac{\varepsilon_k}{4 v_F^2} \frac{D^2}{\rho_m v_{ph}^2} k_B T. \tag{8}$$

Thus, in the nondegenerate EP regime ($\hbar \omega_q \ll k_B T$), the scattering rate $[1/\tau(\varepsilon_k)]$ depends linearly on the temperature. Since at low temperatures ($T_{BG} \ll T \ll E_F / k_B$) $\langle \tau \rangle \approx \tau(E_F)$, the calculated conductivity is independent of Fermi energy or equivalently the electron density. Therefore, the electronic mobility in graphene is inversely proportional to the carrier density, i.e., $\mu \propto 1/n$. The EP regime has recently been considered in the literature.[18,19] We note that the similar linear temperature dependence of the scattering time has been reported for nanotubes[20] and graphites.[21]

To calculate the relaxation times in the BG regime where $\hbar \omega_q \sim k_B T$, we have to keep the full form as in Eq. (5). Since the acoustic phonon energy is comparable to $k_B T$, the temperature dependence of the relaxation time via the statistical occupation factors in Eq. (5) becomes more complicated. In BG regime, the scattering rate is strongly reduced by the occupation factors because for phonon absorption, the phonon population decreases exponentially and also phonon emission is prohibited by a sharp Fermi distribution. To calculate the low-temperature behavior of the resistivity, we can rewrite the averaged inverse scattering time over energy as

$$\frac{1}{\langle \tau \rangle} = \frac{1}{2\pi\hbar} \frac{2 E_F}{(\hbar v_F)^2} \int dq (1 - \cos\theta) |C(q)|^2 G(\omega_q), \tag{9}$$

where $q = 2 k_F \sin(\theta/2)$ and $G(\omega)$ is given by[22]

$$G(\omega) = \frac{1}{k_B T} \int d\varepsilon f(\varepsilon) \{ N_q [1 - f(\varepsilon + \omega)] + (N_q + 1)[1 - f(\varepsilon - \omega)] \} = \frac{2\omega}{k_B T} N_q (N_q + 1). \tag{10}$$

Then, we have in low-temperature limits $T \ll T_{BG}$,

$$\frac{1}{\langle \tau \rangle} \approx \frac{1}{\pi} \frac{1}{E_F} \frac{1}{k_F} \frac{D^2}{2 \rho_m v_{ph}} \frac{4! \zeta(4)}{(\hbar v_{ph})^4} (k_B T)^4. \tag{11}$$

Thus, we find that the temperature-dependent resistivity in BG regime becomes $\rho \sim T^4$ without screening effects. If we include screening effects by the carriers themselves,[23] the low-temperature resistivity goes as $\rho \sim T^6$. The screening effects on the bare scattering rates can be introduced by dividing the matrix elements $C(q)$ by the dielectric function of graphene. However, the matrix elements in graphene arise from the change in the overlap between orbitals placed on different atoms and not from a Coulomb potential. Thus, we neglect screening effects in the calculation and only consider unscreened deformation-potential coupling. Even though the
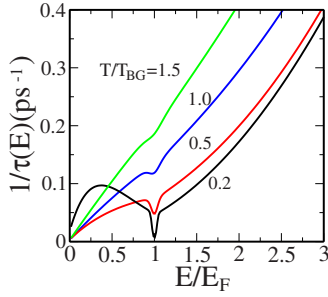
FIG. 1. (Color online) Calculated inverse relaxation times as a function of energy for different temperatures T/T_{BG}=0.2, 0.5, 1.0, and 1.5 for an electron density $n=10^{12}$ cm^{-2} with T_{BG}=54 K. The deformation-potential coupling constant $D=19$ eV and the phonon velocity $v_{ph}=2\times10^6$ cm/s are used in this calculation.

resistivity in EP regime is density independent, Eq. (11) indicates that the calculated resistivity in BG regime is inversely proportional to the density, i.e., $\rho_{BG}\sim1/n$, or equivalently the mobility in BG regime is density independent.

III. RESULTS

In this calculation, we use the following parameters: graphene mass density $\rho_m=7.6\times10^{-8}$ g/cm^2, acoustic phonon velocity $v_{ph}=2\times10^6$ cm/s, and deformation potential $D=19$ eV. Even though the phonon velocity v_{ph} is well defined experimentally, the value of the deformation-potential coupling constant is not established.[21,24] In general, the constant D could be obtained on the basis of the fact that the shift of energy dispersion from its equilibrium state reaches the order of the atomic energy, i.e., $D\sim e^2/a$, with a being the lattice constant, which is of the order of 10 eV in graphene. We note that we have used Ref. 24 for obtaining the phonon parameters, but different values of D, differing by a factor of 3 (i.e., $D\approx10$–30 eV), are quoted[19,21,24] in the literature. Since $\tau^{-1}\propto D^2$, the resulting graphene resistivity could differ by an order of magnitude depending on the precise value of D.

In Fig. 1, we show the calculated inverse relaxation times for deformation-potential scattering by acoustic phonon as a function of energy for different temperatures T/T_{BG}=0.2, 0.5, 1.0, and 1.5 for an electron density $n=10^{12}$ cm^{-2} with T_{BG}=54 K. The inverse relaxation time in BG regime ($T<T_{BG}$) shows a characteristic dip (suppression of scattering rate) in a narrow region around Fermi energy E_F due to the statistical occupation factors. Above Bloch–Grüneisen temperature ($T>T_{BG}$), the dip structure disappears and the scattering rate becomes close to the scattering rate of equipartition regime.

In Fig. 2(a), we show our calculated graphene resistivity, $\rho\equiv\sigma^{-1}$, as a function of temperature on a log-log plots, clearly demonstrating the two different regimes: BG, $\rho\sim T^4$ behavior for $T<T_{BG}\sim20$–100 K and the EP, $\rho\sim T$ behavior for $T>100$ K. We note that T_{BG} ($\propto\sqrt{n}$) depends weakly on density, and the true BG behavior is likely to show up at relatively low temperatures. In Fig. 2(b), we show $\rho(T)$ for several densities on a linear plot, emphasizing the strong
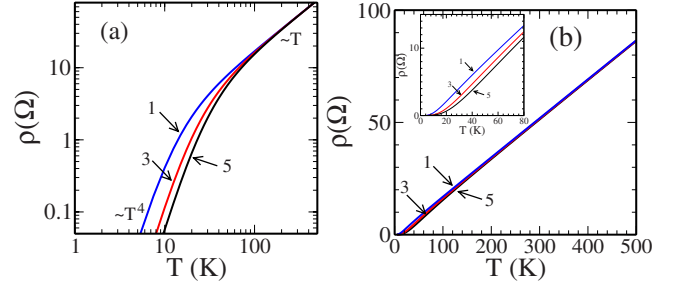
FIG. 2. (Color online) (a) Calculated graphene resistivity as a function of temperature for several densities $n=1\times10^{12}$, 3×10^{12}, and 5×10^{12} cm^{-2}. We use the deformation potential $D=19$ eV. Note that in BG regime ($T<T_{BG}$), $\rho\sim T^4$ and in EP regime ($T>100$ K), $\rho\sim T$. (b) The same as (a) in linear scale. The inset shows the resistivity in low-temperature limits ($T<80$ K).

linear in T dependence of the acoustic phonon-limited graphene resistivity ranging from 100 to 500 K. This rather large temperature range of $\rho(T)\sim T$ behavior of acoustic phonon scattering limited resistivity is quite generic to 2D semiconductor structures, and our finding for graphene here is qualitatively similar to what was earlier found to be the ease for 2D GaAs structures.[15,16] The crucial difference between graphene and 2D GaAs is that in the latter system polar optical phonon scattering becomes exponentially more important for $T\gtrsim100$ K and dominates at room temperatures, whereas in graphene, we predict a linear 2D resistivity up to very high temperatures (~1000 K) since the relevant optical phonon has very high energy (~2000 K) and is simply irrelevant for carrier transport.

In Fig. 3, we show our calculated intrinsic graphene mobility, $\mu\equiv(en\rho)^{-1}$, as functions of temperature and carrier density. Within our model, the unscreened acoustic phonon scattering limited graphene mobility is inversely proportional to T and n individually for $T\gtrsim100$ K. Assuming $D=19$ eV, as used in Fig. 3, μ could reach values as high as 10^5 cm^2/V s for lower carrier densities ($n\lesssim10^{12}$ cm^{-2}). For larger (smaller) values of D, μ would be smaller (larger) by a factor of D^2. It may be important to emphasize here that we know of no other system where the intrinsic room-temperature carrier mobility could reach a value as high as 10^5 cm^2/V s.
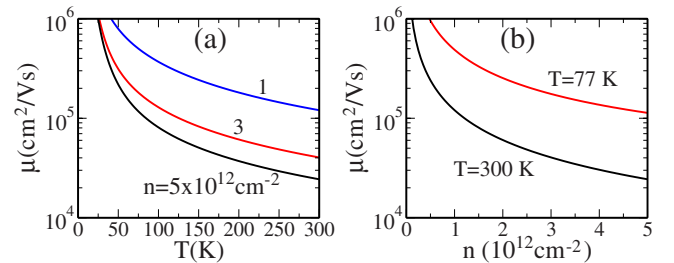
FIG. 3. (Color online) Calculated mobility limited by the acoustic phonon with the deformation-potential coupling constant $D=19$ eV (a) as a function of temperature for different densities $n=1\times10^{12}$, 3×10^{12}, and 5×10^{12} cm^{-2} and (b) as a function of density for different temperatures $T=77$ K and $T=300$ K.

IV. DISCUSSION

The three key theoretical findings on phonon-limited graphene mobility of this work are: (1) $\rho \sim T$ for $T \gtrsim 100$ K, (2) $\rho \propto T^4$ (T^6) for $T \lesssim 50$ K, for unscreened (screened) deformation-potential coupling, and (3) $\mu \gtrsim 3.7 \times 10^7 / D^2 \tilde{n}$ cm^2/V s, at room temperature ($T = 300$ K) where D is measured in eV and $\tilde{n}$ is carrier density n measured in units of 10^{12} cm^{-2}. These theoretical predictions being rather precise, the question naturally arises about the experimental status and the verification of our theory. Very recently, experimental graphene transport data at room temperature (or even above[17]) have started becoming available.[17,18] The only aspect of our theory that can be directly compared with the existing experiment is the $\rho \propto T$ behavior at high temperatures (>200 K), and this is indeed consistent with the recent data from two different groups.[17,18] Geim and co-workers have recently concluded[18] that the room-temperature graphene intrinsic mobility could be as high as 10^5 cm^2/V s, which is also consistent with our theory. However, as emphasized by us, the actual mobility value varies inversely as D^2, and therefore a precise knowledge of the deformation-potential coupling is required for an accurate estimate of the intrinsic mobility.

A more detailed comparison between our theory and the experimental results on $\rho(T)$ shows some qualitative difference, which are not understood at this point. For example, the experimental crossover[17,18] to the high-temperature linear ($\rho \sim T$) behavior in the intrinsic resistivity appears to be closer to a T^2 behavior rather than the T^4 BG behavior we predict. More disturbingly, the experimental crossover from the high-temperature linear behavior to the low-temperature high power law behavior appears to be occurring at a much higher temperature (100–200 K) than the theoretical prediction (20–50 K). At this stage, we have no explanation for the lower-temperature disagreement between experiment and theory, but below we discuss several possibilities.

The experimentally measured resistivity in the current graphene samples is completely dominated by extrinsic scattering (and *not* by phonon scattering) even at room temperatures, since the low-temperature ($\lesssim 4$ K) mobility is typically 5000–15 000 cm^2/V s, and the intrinsic room-temperature phonon contribution, as obtained theoretically by us or inferred[17,18] from recent temperature-dependent experiments, is 10–20 times larger ($\sim 100\,000$ cm^2/V s). This means that any experimental extraction of the pure phonon contribution to graphene resistivity involves subtraction of two large resistances (i.e., the measured total resistance and the extrapolated $T = 0$ extrinsic temperature-independent resistance arising from impurity and defect scattering) of the order of kiloohms each to get a phonon contribution roughly of the order of 100 Ω. Apart from the inherent danger of large unknown errors involved in the subtraction of two large numbers to obtain a much smaller number associated with phonon scattering contribution to graphene mobility, there is the additional assumption of the Matthiessen rule, i.e., $\rho_{tot} = \rho_{ph} + \rho_i$, where ρ_{tot} is the total resistivity contributed by impurities and defects (ρ_i) and phonons (ρ_{ph}), which is simply not valid. In particular, the impurity contribution to resistivity also has a temperature dependence arising from Fermi statistics and
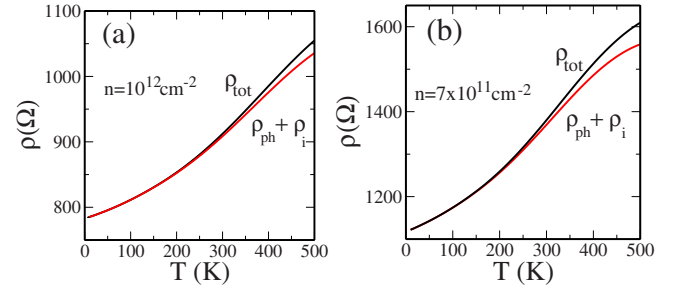
FIG. 4. (Color online) The deviations from Matthiessen's rule for two different densities, (a) $n = 10^{12}$ cm^{-2} and (b) $n = 7 \times 10^{11}$ cm^{-2}. Here, ρ_i (ρ_{ph}) represents the resistivity due to impurity (phonon) scattering.

screening which, although weak, cannot be neglected in extracting the phonon contribution (particularly since the total phonon contribution itself is much smaller than the total extrinsic contribution). In particular, the temperature-dependent part of the charged impurity scattering contribution to graphene resistivity could be positive or negative[25] depending on whether screening or degeneracy effects dominate, and therefore the phonon contribution, as determined by a simple subtraction, could have large errors, particularly in the low ($T < 1000$ K) temperature regime. Indeed, a recent measurement[26] of $\rho(T)$ in the 0–100 K regime finds small temperature-dependent contributions to graphene resistivity which could be either positive or negative depending on the sample mobility and which, in all likelihood, arises from extrinsic impurity scattering.

In Fig. 4, we show the failure of the Matthiessen rule in graphene (particularly at higher and/or lower temperatures and/or densities) by calculating the total graphene resistivity arising from screened charged impurity scattering (ρ_i) and phonon scattering (ρ_{ph})—it is clear that $\rho_{tot} \neq \rho_{ph} + \rho_i$ for lower and/or higher densities and/or temperatures.

If the experimentally extracted[17,18] phonon contribution to the graphene resistivity turns out to be accurate in spite of the rather questionable subtraction procedure discussed above, then the disagreement between our intermediate temperature (50–100 K) theoretical results and the experimental data would indicate the presence of some additional phonon modes which must be participating in the scattering process. We can, in fact, get reasonable agreement between our theory and the experimental data by arbitrarily shifting the BG temperature T_{BG} to a higher temperature around 200 K. This shift could indicate a typical phonon scale which causes additional scattering other than the LA phonons coupled to the carriers through the deformation-potential coupling considered in our work. At this stage, we cannot speculate on what these additional modes could be. One possibility is that these are the zone-edge out of plane acoustic (ZA) phonon modes with vibrations transverse to the graphene plane.[17] (In Appendix, we provide the calculated carrier resistivity in the presence of an additional phonon mode with a soft gap.) Another possibility considered in Ref. 18 is that these are the thermal fluctuations ("ripplons") of the mechanical ripples invariably present in graphene samples.[10] Of course such additional "phonon" scattering channels will lead to additional unknown coupling parameters making the resultant theory

essentially a data fitting procedure. The advantage of our minimal theory is that it involves only two phonon parameters: D and v_{ph} associated with the 2D graphene LA phonons. More data in higher-mobility samples will be needed to settle this question since the subtraction problem inherent in the current technique for extracting the phonon contribution would make analyzing this issue a difficult task.

V. CONCLUSION

We have calculated the intrinsic temperature-dependent 2D graphene transport behavior up to 500 K by considering temperature and density-dependent scattering of carriers by acoustic phonons. We have provided a critical discussion of our results in light of the recent experiments.[17,18] The lack of precise quantitative knowledge about graphene deformation-potential coupling makes a quantitative comparison with the experimental data problematic.

ACKNOWLEDGMENTS

APPENDIX

In this Appendix, we calculate the phonon scattering limited carrier mobility including effects of two phonon branches: the regular LA phonon (as considered in the main part of this paper) and an additional "intervalley" phonon branch with a soft gap ($\sim$70 meV) representing the intervalley phonon, the ZA phonon mode at the K point. The theoretical motivation is to demonstrate that the combination of the LA phonon and an optical phonon (i.e., the intervalley ZA mode) with a softy gap could indeed lead to qualitative (or even quantitative, if the phonon parameters have appropriate values) agreement between theory and experiment.

In this context, we consider the long wavelength phonon scattering. As temperature increases, phonons of large wave vectors are involved in the scattering in multivalley structures. Thus, the intervalley phonon scattering becomes significant at high temperatures.[17] In graphene, there are two minima of the conduction band at K and K' points in the Brillouin zone. The scattering between K and K' points requires the participation of intervalley phonons, whose wave vectors are close to $\mathbf{q}_{ij} = \mathbf{k}_K - \mathbf{k}_{K'}$ and the frequencies of these phonons are close to $\omega_{ij} = \omega(q_{ij})$. The relaxation time for intervalley phonon scattering may be considered by assuming
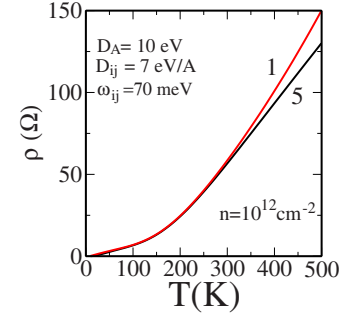
FIG. 5. (Color online) Calculated resistivity with both the acoustic phonon scattering and the intervalley phonon scattering. See Appendix for details.

constant intervalley phonon energies $\hbar\omega_{ij}$. Then, the matrix element for the intervalley phonon scattering becomes $|C(\mathbf{q})|^2 = \hbar D_{ij}^2 / 2A\rho_m\omega_{ij}$, where D_{ij} is the deformation-potential coupling constant for intervalley phonons in unit of eV/Å. Since $\omega_{ij} \ll E_F$ in graphene, the scattering of electrons from intervalley phonons is considered quasielastically.

In Fig. 5, we show the calculated resistivity with both the acoustic phonon scattering and the intervalley phonon scattering as a function of temperature for two different densities. The following parameters are used in this calculation: deformation-potential coupling constant $D = 10$ eV, acoustic phonon velocity $v_{ph} = 2 \times 10^6$ cm/s, $D_{ij} = 7$ eV/Å, and intervalley phonon energy $\hbar\omega_{ij} = 70$ meV which corresponds to the lowest phonon energy (ZA) at the K point. The calculated resistivities have very weak density dependence, which comes from the energy averaging. Below 200 K, the acoustic phonon scattering dominates (linear in temperature), but above 200 K, both phonon scatterings contribute in the transport. Note that the temperature dependence of the resistivity is linear in both regimes, but has different slopes. The high power law behavior ($\rho \sim T^4$) only applies at very low temperatures ($T < 50$ K). Basically, there is a sharp turn on in phonon scattering in the 150–250 K range as the intervalley ZA phonon scattering becomes effective.

Whether the results shown in Fig. 5 including the effects of intervalley phonon scattering are physically meaningful or not will depend on the direct observation of these ZA phonon modes via Raman scattering experiments. At this stage, all we have established is that inclusion of this additional soft-gap phonon mode gives impressive agreement between theory and experiment.[17,18] More work is needed to validate the model of combined LA and ZA phonon scattering contributing to the temperature-dependent graphene resistivity.

[1] K. S. Novoselov, A. K. Geim, S. V. Morozov, D. Jiang, Y. Zhang, S. V. Dubonos, I. V. Grigorieva, and A. A. Firsov, Science **306**, 666 (2004).

[2] Y. Zhang, Y.-W. Tan, H. L. Stormer, and P. Kim, Nature (London) **438**, 201 (2005).

[3] Y.-W. Tan, Y. Zhang, K. Bolotin, Y. Zhao, S. Adam, E. H. Hwang, S. Das Sarma, H. L. Stormer, and P. Kim, Phys. Rev. Lett. **99**, 246803 (2007).

[4] J. H. Chen, C. Jang, M. S. Fuhrer, E. D. Williams, and M. Ishigami, arXiv:0708.2408 (unpublished).

[5] See, for example, the special issues, Solid State Commun. **143**, 1 (2007); Eur. Phys. J. Spec. Top. **148**, 1 (2007).

[6] T. Ando, J. Phys. Soc. Jpn. **75**, 074716 (2006).

[7] K. Nomura and A. H. MacDonald, Phys. Rev. Lett. **96**, 256602 (2006).

[8] V. V. Cheianov and V. I. Fal'ko, Phys. Rev. Lett. **97**, 226801 (2006).

[9] E. H. Hwang, S. Adam, and S. Das Sarma, Phys. Rev. Lett. **98**, 186806 (2007).

[10] S. Adam, E. H. Hwang, V. M. Galitski, and S. Das Sarma, Proc. Natl. Acad. Sci. U.S.A. **104**, 18392 (2007); V. M. Galitski, S. Adam, and S. Das Sarma, Phys. Rev. B **76**, 245405 (2007); E. H. Hwang, S. Adam, and S. Das Sarma, *ibid.* **76**, 195421 (2007); S. Adam, E. H. Hwang, and S. Das Sarma, Physica E (Amsterdam) **40**, 1022 (2008).

[11] T. Ando, A. B. Fowler, and F. Stern, Rev. Mod. Phys. **54**, 437 (1982).

[12] M. J. Manfra, E. H. Hwang, S. Das Sarma, L. N. Pfeiffer, K. W. West, and A. M. Sergent, Phys. Rev. Lett. **99**, 236402 (2007).

[13] H. Stormer (private communication); E. D. Williams (private communication); A. Geim (private communication).

[14] L. Pfeiffer (private communication).

[15] T. Kawamura and S. Das Sarma, Phys. Rev. B **45**, 3612 (1992).

[16] T. Kawamura and S. Das Sarma, Phys. Rev. B **42**, 3725 (1990).

[17] M. Fuhrer (private communication).

[18] A. Geim (private communication); S. V. Morozov, K. S. Novoselov, M. I. Katsnelson, F. Schedin, D. Elias, J. A. Jaszczak, and A. K. Geim, Phys. Rev. Lett. **100**, 016602 (2008).

[19] T. Stauber, N. M. R. Peres, and F. Guinea, Phys. Rev. B **76**, 205423 (2007); F. T. Vasko and V. Ryzhii, *ibid.* **76**, 233404 (2007).

[20] C. L. Kane, E. J. Mele, R. S. Lee, J. E. Fischer, P. Petit, H. Dai, A. Thess, R. E. Smalley, A. R. M. Verschueren, S. J. Tans, and C. Dekker, Europhys. Lett. **41**, 683 (1998).

[21] L. Pietronero, S. Strässler, H. R. Zeller, and M. J. Rice, Phys. Rev. B **22**, 904 (1980); L. M. Woods and G. D. Mahan, *ibid.* **61**, 10651 (2000); H. Suzuura and T. Ando, *ibid.* **65**, 235412 (2002); G. Pennington and N. Goldsman, *ibid.* **68**, 045426 (2003).

[22] P. J. Price, J. Appl. Phys. **53**, 6863 (1982).

[23] E. H. Hwang and S. Das Sarma, Phys. Rev. B **75**, 205418 (2007).

[24] S. Ono and K. Sugihara, J. Phys. Soc. Jpn. **21**, 861 (1966); K. Sugihara, Phys. Rev. B **28**, 2157 (1983).

[25] E. H. Hwang and S. Das Sarma (unpublished).

[26] Y.-W. Tan, Y. Zhang, H. L. Stormer, and P. Kim, Eur. Phys. J. Spec. Top. **148**, 15 (2007).